Egypt. J. Chem. **Vol. 65,** No. SI:13B pp. 617- 627 (2022)

Egyptian Journal of Chemistry

http://ejchem.journals.ekb.eg/

Geochemical Characterization of the Upper Cretaceous Duwi Phosphorites in the Beida Mine, Central Eastern Desert, Egypt: Implications of P_2O_5 – F – U Interrelations.

Aya Osham[1], Abdel Moneim Mahmoud[1] Mohamed Abdel Aal[1], Ahmed Gad[2], Weal Abdel Wahab[3]

1- Biological and Geological Sciences Department, Faculty of Education, Ain Shams University, Cairo 11341, Egypt.

2- Geology Department, Faculty of Science, Ain Shams University, Cairo 11566, Egypt.

3- Geological Sciences Department, National Research Centre, Dokki, Cairo 12622, Egypt.

Abstract

Integrated petrographical, mineralogical and geochemical studies were carried out on the phosphate beds of the Duwi Formation, which was exposed at the Beida mine. Petrographically, the investigated phosphatic microfacies are Molluscal bioclastic phosphatic grainstone and Biopeloidal phosphatic grainstone, generally composed of phosphatic pellets of collophane and bioclasts bone and teeth fragments indicating a high-energy near-shore depositional environment and formed authigenically within oxic to suboxic zones from phosphate-rich sediments. The main mineralogical constituents of the considered sample are phosphatic minerals including dahlite, francolite and hydroxylapatite, while the non-phosphatic minerals are quartz, calcite, halite and ankerite. Geochemical studies reflect that the phosphorites in the Beida mine obtain medium-grade ore with an average of 25.01 % P_2O_5. The significant correlation between P_2O_5 and U reflects that the U may be present in the apatite crystal lattice. The more considerable values in the calculated uranium rather than measured uranium could be attributed to the post-depositional enrichment of uranium.

Keywords: Duwi, Beida, Phosphate, Fluorine, Uranium, Geochemistry.

INTRODUCTION

Phosphorite is a non-renewable resource without a substitute and significant raw material for phosphatic fertilizers and phosphorus-based chemicals [1-3]. Sedimentary phosphate deposits are a type of bio-elemental chemical sedimentary rock that contains high concentrations of the nutrient elements P, Fe, and/or Si [4,5]. Sedimentary phosphorite deposits of different ages are widely distributed throughout the world with major economic concentrations located in the United States, Morocco, China, Russia, South Africa, Jordan, and Australia. In the Middle East and surrounding countries, commercial phosphorite deposits are extending from Morocco in the West to Iraq and Turkey in the East passing through Algeria, Tunisia, Egypt, Syria, Jordan, and Saudi Arabia [6]. The phosphate occurrences in Egypt from north to south were subdivided into three east-west trending facies belts; that are northern, central, and southern facies. The central facies belt represents the most economic occurrences and includes three major localities; the Red Sea Region, on both sides of the Nile Valley (East and West El Sibaiya area - Abu Had - Wadi Hamama), and Western Desert (Abu Tartur - Dakhla Plateau) [7]. Marine phosphorites are usually hosted significant U contents in the range of 50 - 200 ppm [8]. Uranium ions can be fixed in apatite, the inclusion of uranium in the apatite lattice is certainly not by displacement of Ca^{+2} ions from the lattice, but during the formation of apatite lattice when $CaCO_3$ interacts with a phosphate-rich solution to form apatites [9]. The Egyptian phosphorites demonstrate a positive correlation between P-U, U-V, and P-F, while a negative correlation between the P-Ca and U-S [10]. The phosphate rocks of marine sedimentary origin contain elevated concentrations of heavy metals, radioactive elements, and rare earth elements [11].

Corresponding Author: Ayaosham@Edu.Asu.Edu.eg

Receive Date: 28 April 2022, Revise Date: 17 May 2022, Accept Date: 25 May 2022

DOI: 10.21608/EJCHEM.2022.136420.6011

The main purpose of this study is to apply Microfacies analysis, mineral characteristics and a standard geochemical technique to understand the depositional environment and degree of uranium enrichment of the Beida mine phosphorites.

MATERIAL AND METHODS

STUDY AREA

The study area is located in the central part of the Eastern Desert. In the Beida mine, the Upper Cretaceous Duwi Formation is located about 1.4 km north of the Qift - Quseir road and coordinates; latitude. 26° 06' 35.7" N and longitude: 34° 05' 13.1" E (Fig. 1).

GEOLOGIC SETTING

The exposed sedimentary succession in the study area was discussed by [12], [13], [14], [15], [16], [17], [18]. Fig. 2 shows the geological map of the study area. The Duwi Formation attains 66 meters thick in its type section at Gabal Duwi, Quseir area. Duwi Formation was termed by [14], [16], [19] in Gebel Duwi, west of Quseir, Red Sea Coast. The rock unit conformably overlies the Quseir Variegated Shale and underlies the Dakhla Shale. The Duwi Formation is composed of hard semicrystalline or siliceous limestones, marls and several phosphatic bands. The Duwi Formation is assigned to Campanian to Maastrichtian age [15]. The fossiliferous carbonates of the Duwi Formation include some Ammonites and other Molluscan faunas in addition to some shark teeth [14]. In the Beida mine, the Duwi Formation is composed of varicolored shale (grey, green, greenish grey) intercalated with phosphatic beds at the middle and upper members of the Duwi Formation (yellow, white), grey fissile siliceous shale, yellow hard sandstone, argillaceous sandstone and highly fractured yellow limestone at the upper part. The total thickness of the Duwi Formation in the Beida mine is 51 m (Fig. 3).

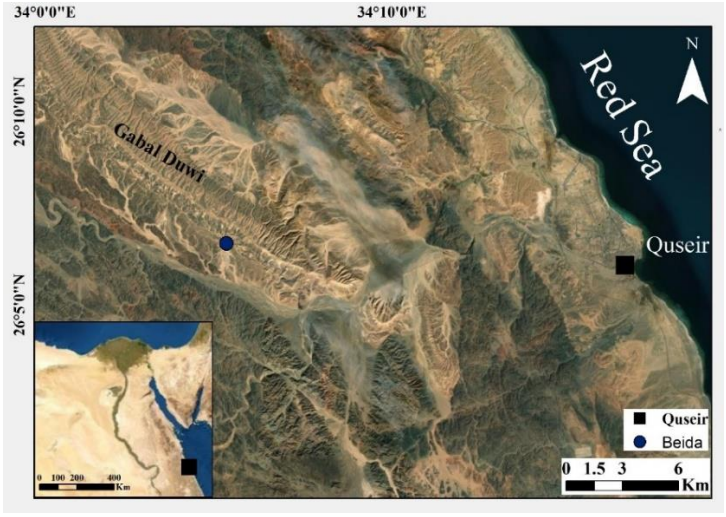

Fig. 1: Location map of the study area.

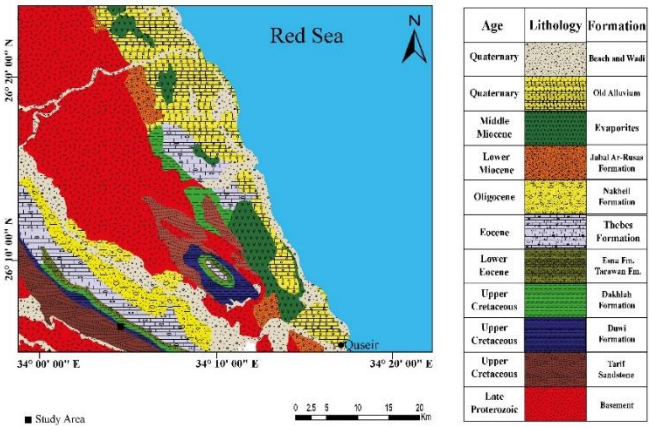

Fig. 2: Geological map of the study area, modified after The Egyptian Survey and Mining Authority (1992).

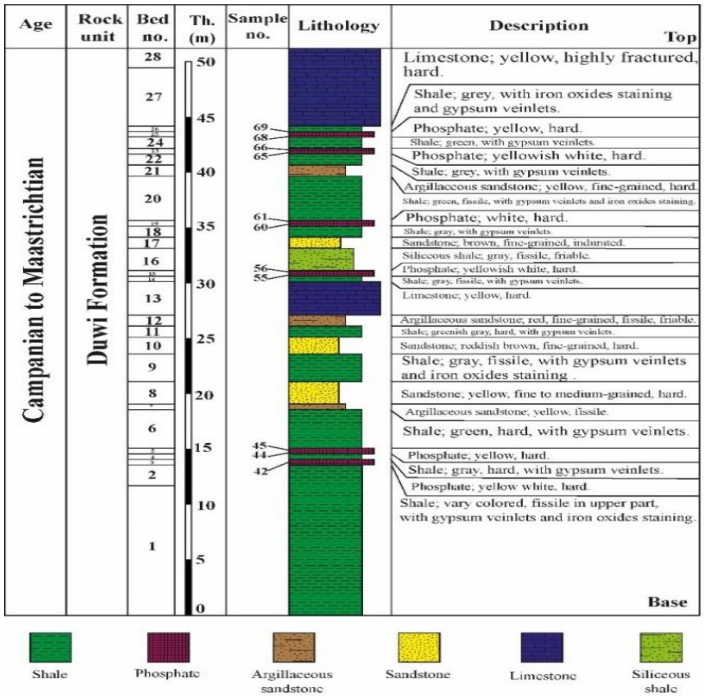

Fig. 3: The stratigraphic columnar section of the Duwi Formation in the Beida mine.

METHODOLOGY

Eleven representative phosphate samples were collected from the Duwi Formation in the Beida mine. Petrographically, four phosphate samples were selected, and their thin sections were examined under the polarizing microscope to identify the microfacies association based on Pettijohn [20] and Dunham [21] classifications. Mineralogically, the X-ray diffraction pattern for the phosphate sample no. 56 was investigated by using a BRUKER-D8 Advanced diffractometer with Ni filter, Cu-Kα radiation available at the National Research Center, Egypt. Instrument settings were 40 Kv and 40 mA potential, scanning speed of 0.02º/S and the 2θ ranged between 40 to 60º. Geochemically, Major and trace elements of eleven phosphate samples were determined by X-ray fluorescence (XRF) technique using Axios Sequential WD-XRF Spectrometer, PANalytical (2021) according to the ASTM E-1621 standard guide for elemental analysis by wavelength-dispersive X-ray fluorescence Spectrometer and the ASTM D-7348 standard test method for loss on ignition (L.O.I.) on solid combustion, which was used as guidelines to detect quantitative determination of major and trace element concentrations in selected samples.

RESULTS AND DISCUSSION

PETROGRAPHY

The recorded microfacies of the studied phosphate samples in the Beida mine are:

1. Molluscal bioclastic phosphatic grainstone

This microfacies is recorded only in the middle member of the Duwi Formation in the Beida mine (samples no. 55 and 56). It is composed of phosphatic pellets of collophane and bioclasts (bone, teeth, and oyster shell fragments) compose about 30 – 40 % of the thin section (Fig. 4a). The phosphatic pellets are variable in shape (subrounded to subangular) with various sizes from 0.2 to 1 mm. These pellets are poorly sorted and disoriented. The bioclastic grains are represented by longitudinal vertebrate bone fragments and oyster shell fragments. These skeletal grains are less than phosphatic pellets. In addition, it contains elongated coprolite grain that reaches 2 mm in diameter. All of these components are embedded in microsparite calcite cement (Fig. 4b).

2. Biopeloidal phosphatic grainstone

This microfacies is recorded in the upper member of the Duwi Formation (samples no. 66 and 68). The phosphatic pellets have a subrounded to subangular and oval shape. These pellets of collophane are poorly sorted and disoriented. The bioclastic grains are represented by fractured vertebrate bone fragments due to compaction and teeth. These phosphatic grains compose about 50 – 60 % of the thin section of various sizes (0.2 - 2 mm). All of them are embedded in microsparite calcite cement (Fig. 4 c, d).

Interpretation

The presence of marine vertebrates (bone fragments) suggests a high-energy near-shore depositional environment. These sediments were deposited in suboxic, protected-shallow basins with moderate water circulation. The peloidal phosphates were formed authigenically in oxic to suboxic zones, from phosphate-rich sediments, followed by storm wave winnowing and storm-generated, shelf-parallel geostrophic currents and minor compaction [22], [23], [24]. The presence of oysters shows shallow marine influences and represents submarine carbonate

skeletal shoals typically forming in a restricted shallow subtidal regime [25].

MINERALOGY

X-ray diffraction pattern of the bulk phosphorite sample (Fig. 5) indicates that the phosphate of the Beida mine is consisted essentially of phosphatic and non-phosphatic minerals, the detected phosphatic minerals are dahlite, francolite, and hydroxylapatite, while the non-phosphatic minerals are quartz, calcite, halite and ankerite (Table 1).

GEOCHEMISTRY

The elemental concentrations and descriptive statistics are listed in Table 2. The treated elements include the major elements as oxides with halogens; SiO_2, Al_2O_3, CaO, MgO, P_2O_5, Fe_2O_3, Na_2O, K_2O, F, Cl, SO_3, and L.O.I.

The analyzed trace elements are As, Ba, Cd, Co, Cr, Cu, Mn, Ni, Pb, Rb, Sr, Ti, V, Y, Zn, Zr, La, Th and U. Correlation coefficients have been used in determining the interrelationships between elements in sediments and have proven to be effective [26]. The correlation coefficients between the analyzed element concentrations are summarized in Table 3.

In the investigated samples, the P_2O_5 ranges between 20.60 – 29.44 % which lies in the average concentration range of major oxides given by Pettijohn [20] (7.14 % - 33.6 %) and is considered an indicator of reducing environment with organic matter or the presence of phosphate minerals as shown in the diffraction analysis.

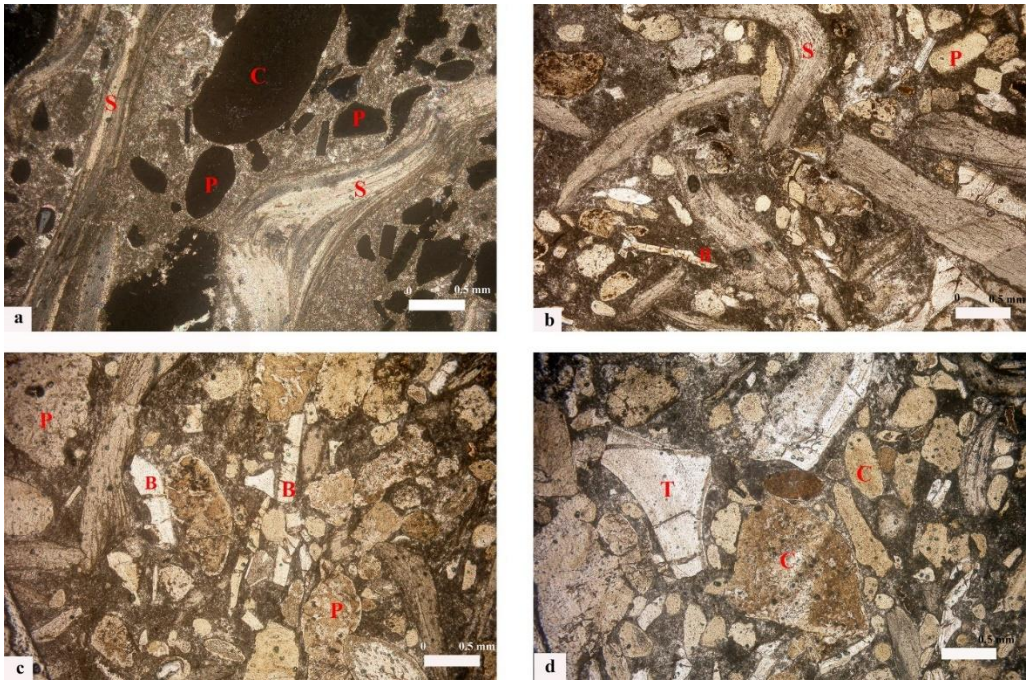

Fig. 4. [a] Photomicrograph showing phosphatic pellets (P), large coprolite (C) and oyster shell fragments (S) embedded in the microsparite calcite cement (XPL), **[b]** Photomicrograph showing vertebrate bone fragments (B), phosphatic pellets (P) and oyster shell fragments (S) (PPL), [**c]** Photomicrograph showing fractured vertebrate bone fragments (B) and phosphatic peloids (P) (PPL), [**d]** Photomicrograph showing teeth fragment (T) and pellets of collophane (C) (PPL).

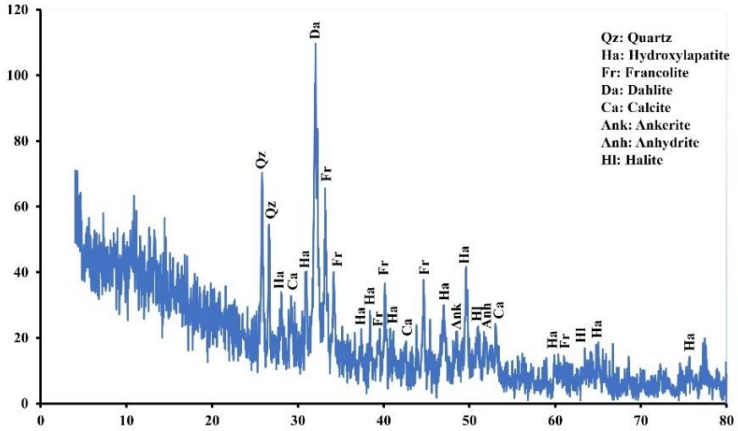

Fig. 5: Representative X-ray diffraction pattern of the phosphate sample no. 56.

Table 1: Minerals detected in XRD analysis of the bulk samples.

Mineral	Chemical Formula	Main lines (A°)	ASTM card
Dahlite	$Ca_5(Po_4,Co_3)_3(OH)$	2.77A°, 3.40A° and 1.72A°	13-1
Francolite	$Ca_5(Po_4,Co_3)_3F$	2.79A°, 2.69A° and 1.62A°	9-432
Hydroxylapatite	$Ca_5(PO_4)_3(OH)$	2.81A°, 2.72A° and 1.84A°	89-1998
Quartz	SiO_2	4.26A° 3.34A°, and 1.82A°	5- 0490
Calcite	$CaCO_3$	3.84A°, 3.03A° and 2.09A°	5-0586
Anhydrite	$CaSO_4$	3.50A°, 2.85A° and 2.33A°	6-0226
Halite	NaCl	3.26A°, 2.82A° and 1.99A°	5-628
Ankerite	$Ca(Fe,Mg,Mn)(CO_3)_2$	2.89A°, 2.90A° and 2.40A°	11-78

The phosphorite ores were subdivided based on their phosphorous content into, high-grade ores (more than 26 % P_2O_5), medium-grade ores (17-26 % P_2O_5) and low-grade ores (less than 16 % of P_2O_5) [27], which mean that the phosphorus in the Beida mine is medium grade ore with an average 25.01 % P_2O_5.

Phosphorous pentaoxide in the phosphate samples exhibits a positive correlation with the major constituent MgO (r = 0.62), and a weak positive correlation with the major constituent CaO (r = 0.35) due to the occurrence of phosphate minerals, while provides a significant negative correlation with major constituent L.O.I. (r = - 0.71). P_2O_5 in the phosphate samples demonstrates a strong to significant positive correlation with the trace elements F (r = 0.86) and U (r = 0.75), The high positive correlation of U with P_2O_5 indicated the important role of phosphate in fixation of U^{6+} as uranyl ion $(UO_2)^{2+}$. Thus, the secondary uranium minerals such as phosphuranylite {$Ca(UO_2)(PO_4)_2(OH)_2\ 6H_2O$}may be precipitated [28], in addition it has a weak positive correlation with the trace element Sr (r = 0.46) and a weak negative correlation with Ti (r = - 0.49) (Fig. 6).

The average CaO/P_2O_5 ratio in the world is given by [29], [30], [31] (about 1.5) which is the same CaO/P_2O_5 ratio in the studied phosphatic samples with an average of 1.75 (Table 4). The moderate trend of the CaO/P_2O_5 indicates the contribution of phosphate is due to precipitation and not by detrital input. High values of P_2O_5 and CaO in the phosphorites of the area indicate more concentration of apatite constituent.

The chemical concentrations of the SiO_2 in the considered phosphate samples with an average of 5.08 % reflect the presence of silica as cement material, which replace the phosphate minerals. The investigated phosphatic samples show high SO_3 content (average 2.03 %), which reflects the presence of anhydrite in the samples, and is confirmed by the appearance of these minerals in the XRD pattern.

The presence of low Al_2O_3 in phosphorites indicates the humid to low temperature climatic conditions at the time of precipitation and phosphatization of these sediments in the area and maybe attributed to minor occurrences of clay minerals. The major content of ferruginous minerals like hematite and ferric-oxides could be related to that these minerals constitute the cementing material of the phosphatic rocks [32].

When marine carbonate and fluorapatite formed, their Sr content was the same (0.24 %), but this concentration was influenced to a great extent by weathering action [29].

P_2O_5, U, Cr, and V are significantly positively correlated. This suggests their association with the francolite structure, while Cd and Ti are significantly negatively correlated with P_2O_5, indicating a common substitution in the francolite structure [33].

The significant correlation between P_2O_5 and U reflects that the U may be present in the apatite crystal lattice and trace elements adsorbed on clay cement. The trace elements in the phosphorite may be present in the apatite lattice or fixed in/or clays [34].

V/Ni ratio higher than 3 indicates that marine origin and organic matter were deposited under reducing conditions, while V/Ni ratios ranging between 1.9 to 3 indicate deposition in a dysoxic-oxic environment with mixed terrigenous and marine organic matter, while V/Ni ratios less than 1.9 indicate predominantly terrigenous organic matter [35]. In the investigated samples, the V/Ni ratio in the phosphatic samples ranges from 1.24 to 5.23 averaging 2.47, which indicates that these phosphatic rocks were deposited under a dysoxic-oxic environment with mixed terrigenous and marine organic matter (Table 4).

P_2O_5 - U - F interrelations

The geochemistry of the Mardin-Mazidag Phosphate deposit was studied by Akyuz et al. [36] using the quadratic regression models of Narula and Wellington [37], which are widely used in many practices to allow the description of the objects in a comparatively wide area of the input variable changes and that is expressed generally as follows:

$$\hat{y} = b_0 + \sum_{i=1}^{m} b_i x_i + \sum_{i=1}^{m} b_i x_i$$

Table 2: The concentrations of the major constituents (in %) of phosphate samples and trace elements (in ppm).

Sample	SiO_2	Al_2O_3	CaO	MgO	P_2O_5	Fe_2O_3	Na_2O	K_2O	F	Cl	SO_3	L.O.I.	As	Ba	Cd	Co
						%							ppm			
42	1.56	0.47	49.59	0.57	29.44	0.79	0.88	0.04	3.22	0.96	0.32	11.98	7.66	58.60	3.40	4.70
44	2.87	0.80	37.82	0.84	21.94	0.51	7.94	0.16	1.20	8.25	1.98	15.50	2.21	29.00	3.50	4.60
45	6.03	0.53	44.06	0.45	23.48	0.89	1.67	0.04	1.57	1.41	2.29	17.42	2.50	33.20	5.80	3.30
55	1.65	0.22	45.55	0.22	25.17	1.13	1.26	0.03	2.72	1.04	1.21	19.66	4.20	28.50	5.10	4.50
56	7.35	0.85	41.62	1.45	28.15	0.81	1.29	0.09	2.98	2.42	3.01	9.84	8.90	8.50	6.50	1.10
60	5.10	0.13	39.78	0.23	23.11	0.26	2.02	0.09	1.99	1.88	3.79	21.32	1.50	17.60	4.30	2.40
61	10.64	0.94	42.04	0.53	20.60	1.37	0.35	0.05	1.01	1.22	2.30	18.75	6.10	7.14	6.60	3.10
65	1.92	0.21	42.17	1.83	28.95	0.83	1.61	0.10	3.02	2.07	1.19	15.48	12.70	7.90	6.00	1.80
66	2.15	1.35	41.57	1.76	27.61	0.26	1.43	0.15	2.39	2.58	6.13	12.27	7.64	24.90	6.70	1.30
68	9.77	0.95	45.01	0.29	22.19	0.79	0.62	0.06	0.98	0.64	0.47	17.87	1.80	12.20	8.10	1.10
69	6.87	0.57	46.32	0.30	24.49	1.10	0.26	0.03	2.67	0.46	0.68	16.07	12.70	13.30	4.40	1.30
Min.	**1.56**	**0.13**	**37.82**	**0.22**	**20.60**	**0.26**	**0.26**	**0.03**	**0.98**	**0.46**	**0.32**	**9.84**	**1.50**	**7.14**	**3.40**	**1.10**
Max.	**10.64**	**1.35**	**49.59**	**1.83**	**29.44**	**1.37**	**7.94**	**0.16**	**3.22**	**8.25**	**6.13**	**21.32**	**12.70**	**58.60**	**8.10**	**4.70**
Ave.	**5.08**	**0.64**	**43.23**	**0.77**	**25.01**	**0.79**	**1.76**	**0.08**	**2.16**	**2.08**	**2.12**	**16.01**	**6.17**	**21.89**	**5.49**	**2.65**

Sample	Cr	Cu	Mn	Ni	Pb	Rb	Sr	Ti	V	Y	Zn	Zr	La	Th	U_m	$U_{calc.}$
								ppm								
42	22.60	6.10	111.60	17.30	4.50	1.40	1135.30	3.70	21.40	21.80	98.30	12.20	3.80	5.60	182.66	49.54
44	49.90	6.70	13.60	14.90	2.20	2.22	788.90	2.99	20.10	3.90	118.40	8.40	1.55	4.70	92.00	46.82
45	35.80	6.90	178.70	17.10	4.60	0.88	885.60	5.30	25.90	29.00	118.20	12.30	7.20	9.10	51.50	47.82
55	20.90	6.60	319.80	13.00	6.40	0.48	824.60	7.90	16.50	15.20	104.30	10.00	15.90	5.40	69.90	41.38
56	71.90	7.40	358.60	14.40	14.90	0.10	969.20	5.90	75.30	42.80	162.20	15.10	28.80	8.60	171.00	48.01
60	97.70	7.80	48.80	33.60	2.50	2.60	754.10	11.00	57.60	26.50	152.20	7.33	14.00	10.50	80.60	42.42
61	29.10	4.50	45.40	6.10	2.10	0.30	568.00	8.00	10.10	12.50	143.60	23.50	5.60	6.90	129.00	44.59
65	86.00	7.20	343.80	15.70	13.30	0.27	761.80	4.40	77.10	44.90	178.70	15.90	32.10	7.10	176.00	50.05
66	73.90	7.20	376.50	18.70	13.60	0.40	914.30	3.40	72.80	37.20	155.90	7.80	25.10	8.00	162.50	52.26
68	25.80	5.00	26.50	7.20	5.80	0.00	1105.50	14.90	18.90	17.00	139.20	14.70	9.40	9.40	79.90	49.83
69	46.40	5.50	13.40	7.40	1.60	0.00	815.20	11.70	13.30	16.50	123.40	13.40	6.80	13.70	124.00	39.78
Min.	**20.90**	**4.50**	**13.40**	**6.10**	**1.60**	**0.00**	**568.00**	**2.99**	**10.10**	**3.90**	**98.30**	**7.33**	**1.55**	**4.70**	**51.50**	**39.78**
Max.	**97.70**	**7.80**	**376.50**	**33.60**	**14.90**	**2.60**	**1135.30**	**14.90**	**77.10**	**44.90**	**178.70**	**23.50**	**32.10**	**13.70**	**182.66**	**52.26**
Ave.	**50.91**	**6.45**	**166.97**	**15.04**	**6.50**	**0.79**	**865.68**	**7.20**	**37.18**	**24.30**	**135.85**	**12.78**	**13.66**	**8.09**	**119.91**	**46.59**

Table 3: Correlation coefficient between major constituents and trace elements of the investigated phosphate samples.

	SiO_2	Al_2O_3	CaO	MgO	P_2O_5	Fe_2O_3	Na_2O	K_2O	F	Cl	SO_3	L.O.I.	As	Ba	Cd	Co	Cr	Cu	Mn	Ni	Pb	Rb	Sr	Ti	V	Y	Zn	Zr	La	Th
Al_2O_3	0.35																												
CaO	-0.05	-0.19																											
MgO	-0.34	0.34	-0.36																										
P_2O_5	-0.61	-0.13	**0.35**	0.62																									
Fe_2O_3	0.42	-0.12	0.47	-0.34	-0.20																								
Na_2O	-0.35	0.03	-0.64	0.12	-0.24	-0.43																							
K_2O	-0.31	0.42	-0.79	0.65	0.06	-0.74	0.67																						
F	-0.59	-0.38	0.42	0.38	**0.91**	-0.03	-0.31	-0.15																					
Cl	-0.31	0.20	-0.71	0.30	-0.17	-0.44	0.97	0.78	-0.27																				
SO_3	-0.11	0.44	-0.59	0.47	0.06	-0.61	0.10	0.64	-0.06	0.23																			
L.O.I.	0.23	-0.46	-0.13	-0.67	**-0.71**	0.18	-0.03	-0.30	-0.51	-0.18	-0.16																		
As	-0.16	-0.02	0.28	0.53	0.63	0.28	-0.38	-0.08	0.69	-0.26	-0.12	-0.52																	
Ba	-0.58	-0.15	0.47	-0.22	0.30	-0.19	0.18	-0.14	0.24	0.08	-0.15	-0.21	-0.23																
Cd	0.55	0.51	-0.07	0.27	-0.10	0.15	-0.46	0.00	-0.31	-0.36	0.21	-0.02	-0.01	-0.59															
Co	-0.44	-0.35	0.13	-0.38	-0.13	0.15	0.44	-0.15	-0.06	0.33	-0.29	0.20	-0.39	0.71	-0.65														
Cr	-0.21	-0.13	-0.62	0.57	0.29	-0.64	0.16	0.60	0.26	0.23	0.59	-0.11	0.23	-0.41	-0.01	-0.49													
Cu	-0.61	-0.32	-0.41	0.45	0.48	-0.68	0.32	0.47	0.45	0.32	0.52	-0.20	-0.02	0.12	-0.25	-0.03	0.73												
Mn	-0.46	0.04	-0.03	0.71	0.70	-0.12	-0.19	0.20	0.60	-0.09	0.41	-0.45	0.37	-0.06	0.31	-0.20	0.32	0.56											
Ni	-0.45	-0.41	-0.34	0.07	0.20	-0.75	0.22	0.33	0.21	0.16	0.50	0.13	-0.30	0.25	-0.38	0.10	0.66	0.80	0.13										
Pb	-0.27	0.25	-0.13	0.85	0.71	-0.25	-0.17	0.37	0.50	-0.03	0.40	-0.62	0.43	-0.23	0.48	-0.48	0.45	0.49	0.90	0.07									
Rb	-0.36	-0.36	-0.39	-0.25	-0.21	-0.58	0.64	0.34	-0.17	0.53	0.17	0.27	-0.55	0.44	-0.69	0.54	0.27	0.43	-0.38	0.74	-0.45								
Sr	-0.15	0.16	0.55	0.01	**0.46**	-0.26	-0.16	-0.13	0.28	-0.19	-0.22	-0.51	-0.07	0.50	0.08	-0.09	-0.26	0.04	0.10	-0.01	0.26	-0.12							
Ti	0.64	-0.10	0.20	-0.62	**-0.49**	0.22	-0.44	-0.47	-0.33	-0.52	-0.31	0.56	-0.20	-0.45	0.33	-0.43	-0.15	-0.45	-0.49	-0.20	-0.38	-0.22	0.04						
V	-0.30	0.04	-0.41	0.81	0.61	-0.57	-0.03	0.55	0.46	0.10	0.60	-0.43	0.33	-0.29	0.24	-0.52	0.86	0.75	0.70	0.52	0.83	-0.02	0.04	-0.33					
Y	-0.20	-0.03	-0.06	0.72	0.71	-0.29	-0.35	0.19	0.56	-0.25	0.40	-0.47	0.47	-0.22	0.36	-0.56	0.64	0.60	0.76	0.34	0.85	-0.29	0.17	-0.28	0.89				
Zn	0.20	0.17	-0.54	0.68	0.19	-0.28	-0.14	0.47	0.05	0.01	0.46	-0.14	0.33	-0.75	0.54	-0.74	0.78	0.31	0.39	0.17	0.63	-0.24	-0.27	0.02	0.80	0.69			
Zr	0.65	0.16	0.17	0.02	-0.17	0.77	-0.45	-0.40	-0.19	-0.37	-0.35	0.00	0.33	-0.45	0.46	-0.18	-0.30	-0.66	-0.11	-0.66	-0.01	-0.58	-0.29	0.18	-0.21	0.00	0.24		
La	-0.25	-0.01	-0.23	0.77	0.63	-0.23	-0.24	0.31	0.53	-0.12	0.41	-0.35	0.47	-0.44	0.43	-0.56	0.65	0.57	0.85	0.21	0.92	-0.37	0.00	-0.20	0.89	0.87	0.77	-0.02	
Th	0.47	-0.02	0.12	-0.23	-0.14	-0.01	-0.46	-0.26	0.02	-0.47	0.05	0.15	0.24	-0.42	0.16	-0.70	0.27	-0.07	-0.26	0.02	-0.14	-0.25	0.00	0.64	0.06	0.17	0.23	0.02	0.03
U	-0.23	0.22	0.15	0.70	**0.75**	-0.05	-0.22	0.22	0.62	-0.05	0.10	-0.76	0.76	0.01	0.00	-0.25	0.29	0.08	0.40	-0.07	0.57	-0.28	0.17	-0.44	0.51	0.52	0.39	0.26	0.48	-0.13

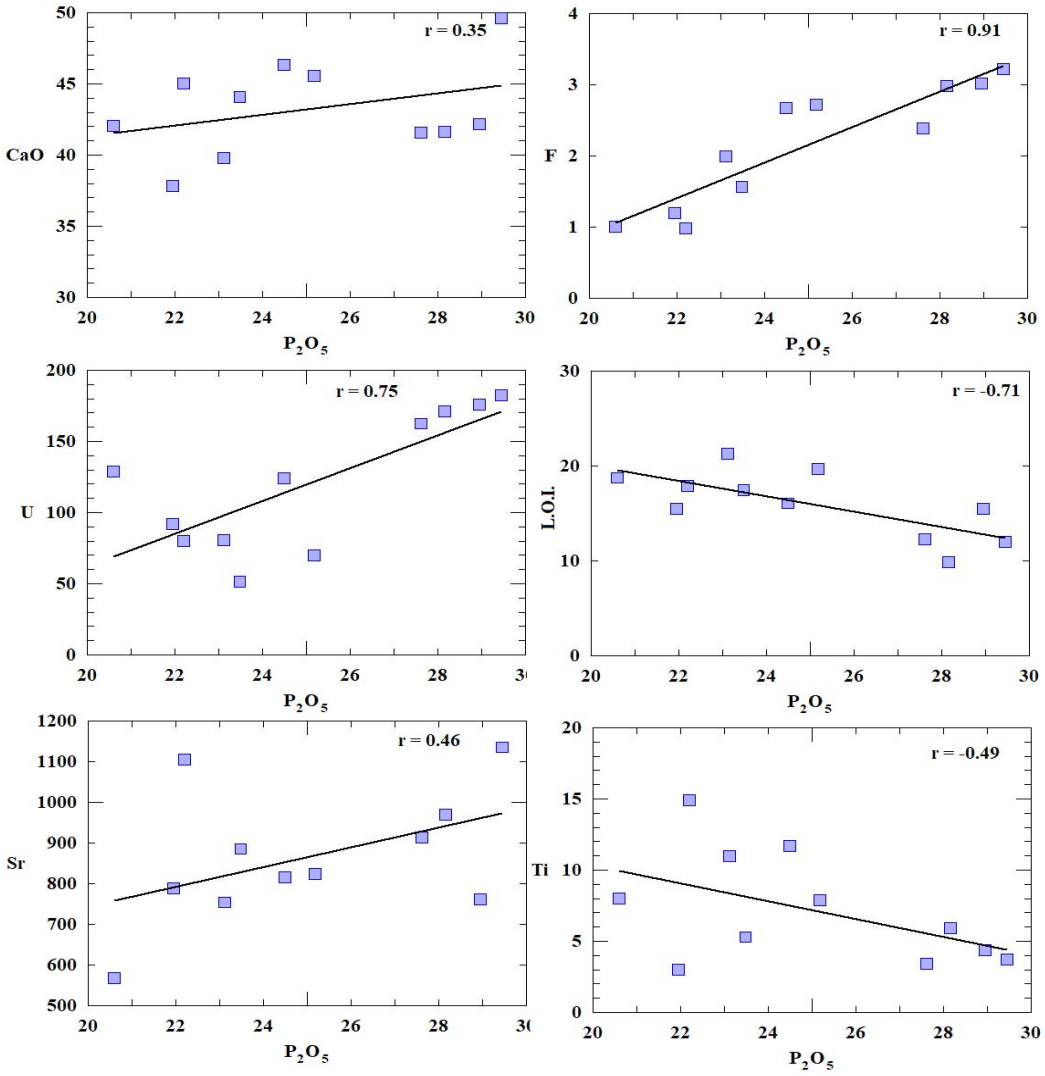

Fig. 6: Binary diagrams between P_2O_5 and other major constituents (in %) and trace elements (in ppm) in the investigated phosphate samples.

Table 4: The average of CaO/P_2O_5 and V/Ni ratios of the studied phosphate samples.

Sample	CaO	P_2O_5	V	Ni	CaO/P_2O_5	V/Ni
42	49.59	29.44	21.40	17.30	1.68	1.24
44	37.82	21.94	20.10	14.90	1.72	1.35
45	44.06	23.48	25.90	17.10	1.88	1.51
55	45.55	25.17	16.50	13.00	1.81	1.27
56	41.62	28.15	75.30	14.40	1.48	5.23
60	39.78	23.11	57.60	33.60	1.72	1.71
61	42.04	20.60	10.10	6.10	2.04	1.66
65	42.17	28.95	77.10	15.70	1.46	4.91
66	41.57	27.61	72.80	18.70	1.51	3.89
68	45.01	22.19	18.90	7.20	2.03	2.63
69	46.32	24.49	13.30	7.40	1.89	1.80
Ave.	**43.23**	**25.01**	**37.18**	**15.04**	**1.75**	**2.47**

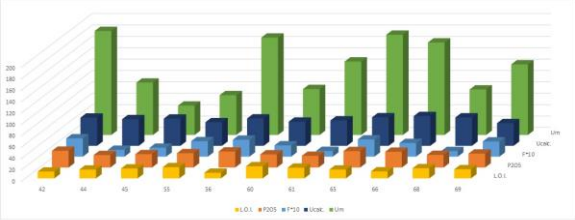

Fig. 7: 3-D plotting showing the Beida mine concentration data series of U_m in ppm, U_{calc} in ppm, P_2O_5 in wt.% and F in wt.%.

Based on real data consisting of Mardin-Mazidag Phosphate deposit observations, Y represents the U concentration in mg/kg and the two predictor variables X_1, X_2 represent P_2O_5 and F concentration in % respectively. The relation between P_2O_5, F and U was distinguished by Akyuz et al. [36] and after the regression analysis for their experiment, the following mathematical model was obtained:

$$\hat{y} = -8.9614 + 3.0972\, x_1 - 10.1493\, x_2$$

As a result, the interrelation between P_2O_5, F and U concentrations of the phosphate ore samples could be expressed as follows:

$$\mathbf{U_{(mg/kg)} = 8.9614 + 3.0972\ P2O5_{(wt.\%)} - 10.1493\ F_{(wt.\%)}}$$

Where U, P_2O_5 and F concentrations represent the Y, X_1 and X_2 respectively in the quadratic regression model. The calculated U(mg/kg) for the Beida mine is presented in Table 2. The 3-D plotting of measured uranium (U_m) in ppm, calculated uranium U_{calc} in ppm, P_2O_5 and F as wt.% shown in (Fig. 7).

The values of the studied samples are higher in U_m values than $U_{calc.}$, which could be attributed to the post-depositional enrichment of uranium [38].

CONCLUSIONS

The present study is concerned with petrography, mineralogy and geochemical characterization of the phosphate beds of the Duwi Formation which was exposed at the Beida mine. The recorded lithofacies of the phosphate samples are Molluscal bioclastic phosphatic grainstone and Biopeloidal phosphatic grainstone. The presence of marine vertebrates suggests a high-energy near-shore depositional environment in suboxic, protected-shallow basins with moderate water circulation. The peloidal phosphates were formed authigenically in oxic to suboxic zones, from phosphate-rich sediments, followed by storm wave winnowing and storm-generated, shelf-parallel geostrophic currents and minor compaction. Also, the presence of oysters shows shallow marine influences.

The X-ray diffraction analysis of the selected sample shows that the phosphatic minerals are dahlite, francolite and hydroxylapatite, while the non-phosphatic minerals are quartz, calcite, halite and ankerite.

Geochemically, the phosphorus in the Beida mine is medium-grade ore with an average of 25.01 % P_2O_5. The moderate trend of the CaO/P_2O_5 indicates the contribution of phosphate is due to precipitation and not by detrital input. The presence of low Al_2O_3 in phosphorites indicates the humid to low temperature climatic conditions at the time of precipitation and phosphatization of these sediments in the area. The positive correlation between P_2O_5, U, Cr, and V suggests their association with the francolite structure, while Cd and Ti are significantly negatively correlated with P_2O_5, indicating a common substitution in the francolite structure. The significant correlation between P_2O_5 and U reflects that the U may be present in the apatite crystal lattice and trace elements adsorbed on clay cement. In the study area, the V/Ni ratio in the phosphatic samples ranges from 1.24 to 5.23 averaging 2.47, which indicated that these phosphatic rocks were deposited under a dysoxic-oxic environment with mixed terrigenous and marine organic matter which is confirmed by the petrographical studies. According to P_2O_5, U and F interrelations based on the quadratic regression models, the values of the studied samples are higher in U_{calc} values than U_m, which could be attributed to the post-depositional enrichment of uranium.

REFERENCES

1. Abouzeid, A.Z.A., Physical and thermal treatment of phosphate ores-An overview, Int. J. Miner. Process, 85, 59–84, (2008).
2. Dos Santos, M.A.; Santana, R.C., Capponi, F.; Ataide, C.H.; Barrozo, M.A.S., Effect of ionic species on the performance of apatite flotation, *Sep. Purif. Technol*, 76, 15–20, (2010).
3. Gharabaghi, M., Irannajad, M., Noaparast, M., A review of the beneficiation of calcareous phosphate ores using organic acid leaching. *Hydrometallurgy*, 103, 96–107, (2010).
4. Pufahl, P.K., Bioelemental sediments. In: James, N.P., Dalrymple, R.W. (Eds.), Facies models, 4th ed., *Geological Association of Canada*, 477–503, (2010).
5. Pufahl, P.K., Groat, L.A., Sedimentary and igneous phosphate deposits: formation and exploration: An Invited Paper. *Econ. Geol*, 112, 483–516, (2017).
6. Ahmed, A.H., Aseri, A.A., Ali, K.A., Geological and geochemical evaluation of phosphorite deposits in northwestern Saudi Arabia as a possible source of trace and rare-earth elements, *Ore Geology Reviews*, 144, (2022).
7. Hermina, M.H., Review on the phosphate deposits of Egypt, *2nd Arab. Conf. Mine, Res. Conf. Paper*, 109-149, (1972).

8. Adams, J.A.S., Osmond, Y.K. and Rogers, J.J.W., The geochemistry of uranium and thorium, *Physics and Chemistry of the Earth*, 3, 298-343, (1959).
9. Ames, L.L., The genesis of carbonate apatite., *Econ. Geol., Dututh.USA*, 827-841, (1959).
10. Tobia, S.K. and Fekry, A.A., Geochemistry of some Egyptian phosphate deposits, *Jour. Geol. U.S.R.*, 8 (1), 11-20, (1964).
11. Hurst, F.J., The recovery of uranium from phosphoric acid: *IAEA, Vienna*, 553p, (1989).
12. Barron, T. and Hume, W.F., Topography and geology of the Eastern Desert of Egypt (Central portion), *Geol. Surv., Dept., Cairo*, 313p, (1902).
13. Beadnell, H.J.L., Report on the geology in the Red Sea Coast between Quseir and Wadi Ranga, Egypt, Mini. Fin, Cairo, *Petro. Res. Ser. Bull*, 13, 37p, (1924).
14. Youssef, M.I., Stratigraphical studies in Quseir area, *Ph.D. Thesis Fac. Sci. Alexandria Univ*, (1949).
15. Youssef, M.I., Upper Cretaceous rocks in Quseir area, Bull. Inst. Desert Egypt, 7 no. 2, 35-53, (1957).
16. Said, R., The geology of Egypt, *Elsevier, Amsterdam, Oxford, New York*, (1962).
17. Abdel Razik, T.M., Stratigraphy of the sedimentary cover of Anz, Atshan South Duwi District, *Bull. Fac. Sci., Cairo Univ.*, no. 41, 153-179, (1967).
18. Abdel Razik, T.M., Comparative studies on the Upper Cretaceous-Early Paleogene sediments on the Red Sea coast, Nile Valley and Western Desert, Egypt, *Proceedings of the 8th Arab Petroleum Congress*, 71, 23p, (1972).
19. Awad, G.H. and Ghobrial, H.G., Zonal stratigraphy of the Kharga Oasis, *Geol. Surv. Egypt*, paper, no.34, 75p, (1965).
20. Pettijohn, F.J., Sedimentary rocks, *Harper & Brothers New York, 3rd Edition*, 628p, (1975).
21. Dunham, R.J., Classification of carbonate rocks according to depositional texture, *Bull. AAPG., Mem.* (1), 108-121, Tulsa / Oklahoma (1962).
22. Glenn, C.R., Follmi, K.B., Riggs, S.R., Baturin, G.N., Grimm, K.A., Trappe, J., Abed, A.M., Galli-Oliver, C., Garrison, R.E., Dyin, A., Jehl, C., Rohrich, V., Sadaquah, R., Schiderlowski, M., Sheldon, R.E. and Seigmund, H., Phosphorus and phosphorites: sedimentology and environments of formation, *Eclogae Geol. Helv*, 87, 747–788, (1994).
23. Pufahl, P.K., Grimm, K.G., Abed, A.M. and Sadaqah, R.M.Y., Upper Cretaceous (Campanian) phosphorites in Jordan: implications for the formation of a south Tethyan phosphorite giant, *Sediment. Geol*, 161, 175–205, (2003).
24. Brookfield, M.E., Hemmings, D.P. and Van Straaten, P., Paleoenvironments and origin of the sedimentary phosphorites of the Napo Formation (Late Cretaceous, Oriente Basin, Ecuador), *J. S. Am. Earth Sci*, 28, 180-192 (2009).
25. Ahmad, F., Farouk, S. and Abd El-Moghny, M.W., A regional stratigraphic correlation for the upper Campanian phosphorites and associated rocks in Egypt and Jordan, *Proceedings of the Geologists' Association*, 125, 419-431, (2014).
26. Liu, W.X., Li, X.D., Shen, Z.G., Wang, D.C., Wai, O.W. H., and Li, Y.S., Multivariate statistical study of heavy metal enrichment in sediments of the Pearl River Estuary, *Environmental Pollution*, 121, 377–388, (2003).
27. Aydin, I., Imamoglu, S., Aydin, F., Saydut, A. and Hamamcim, C., Determination of mineral phosphate species in sedimentary phosphate rock species in sedimentary phosphate rock in Maardin, SE Anatolia, Turkey by sequential extraction, *Jour. Microchem*, 91, 63-69, (2009).
28. Butt, C.R., Mann, A.W. and Horwitz, R.C. Regional setting, distribution and genesis of surficial uranium deposits in calcretes and associated sediments in Western Australia. *Surficial Uranium Deposits, IAEA-TECDOC-322, IAEA, Vienna*, 121-127, (1984).
29. Mcarthur, J.M., Systematic variations in contents of Na, Sr, CO_3, and SO4 in marine carbonate fluorapatite and their relation to weathering, *Chemical geology*, 21 no. (1-2), 89-112, (1978).
30. Mcarthur, J.M., Francolite geochemistry compositional controls during formation, diagenesis, metamorphism and weathering, *Geochimica et Cosmochimica Acta*, 49, 23-35 (1985).
31. Jarvis, I., Burnett, W.C., Nathan, Y., Almbaydin, F.S.M., Attia, A.K.M. Castro, L.N., Flicoteaux, R., Hilmy, M.E., Husain, V., Qutawnah, A.A., Serjani, A. and Zanin, Y.N., Phosphorite geochemistry state of the art and environmental concerns Eclogae Geologicae Helvetiae, *Jour. of the Swiss Geol. Soc.*, 87, 643-700 (1994).
32. Dar, S.A. and Khan, K.F., Depositional Environment of Phosphorites of the Sonari Basin, Lalitpur District, Uttar Pradesh, India, *Applied Studies of Coastal and Marine Environments* 301-319, (2016).
33. Al-Hwaiti, M., Al Kuisi, M., Saffarini, G. and Alzughoul, K., Assessment of elemental distribution and heavy metals contamination in phosphate deposits: potential health risk

assessment of finer-grained size fraction, *Environ Geochem Health*, 36, 651-663, (2014)
34. Lucas, J., Flicoteaux, R., Nathan, Y., Prevot, L. and Shahar, Y., Different aspects of phosphorite weathering. In: Marine phosphorites, *SEPM, SPEC. PUBL.*, 29, 41-51, (1980).
35. Galarraga F., Reategui K., Martïnez A., Martínez M., Llama, J.F., and Márquez, G., V/Ni ratio as a parameter in paleoenvironmental characterization of non-mature medium-crude oils from several Latin American basins, *Journal of Petrological Science and Engineering*, 61, 9-14 (2008).
36. Akyuz T., Akyuz S., Calglar H., and Calgar N., FT-IR, EDXRF Analysis of the Mardin-Mazidag Phosphate Deposit of Turkey and Relations between Phosphate, Uranium and Fluorine, *Asian Journal of Chemistry*, 20 (5), 4085-4091, (2008).
37. Narula S., and Wellington J., Multiple Criteria Linear Regression, *European Journal of Operational. Research*, 181 (2), 767-772, (2007).
38. Abou El-Anwar, E.A. and Ibrahem, W.A., P2O5 - F- U Characterization and Depositional Environment of Phosphatic Rocks for the Duwi Formation, Qussier- Safaga Region, Red Sea Coast, Egypt, *Egyptian Journal of Chemistry*, 62 (12), 2213-2228, (2019).